On the thermodynamic control of ring-opening of 4-substituted 1,3,3-*tris*-carbethoxycyclobutene and the role of C-3 substituent in masking the kinetic torquoselectivity. An alternate reaction pathway

Veejendra K. Yadav, [a]* Dasari L. V. K. Prasad,[a] Arpita Yadav,[b] Maddali L. N. Rao[a]

[a] Department of Chemistry, Indian Institute of Technology, Kanpur 208016, India

[b] Department of Chemistry, University Institute of Engineering & Technology, CSJM University, Kanpur 208024, India

Abstract. The predominant transformations of 4-methyl- and 4-phenyl-1,3,3-*tris*-carbethoxycyclobutenes to s-*trans*,*trans*-1,1,3-*tris*-carbethoxy-4-methyl- and s-*trans*,*trans*-1,1,3-*tris*-carbethoxy-4-phenyl-1,3-butadienes, respectively, are discussed to proceed through pathways entailing heterolytic cleavage of σ_{C3C4} bond rather than the usual conrotatory and disrotatory ring openings following the rules of torquoselectivity. The adventitious or in situ generated halogen acid from $CDCl_3$ catalyzes the reaction by protonation of the geminal ester group to weaken σ_{C3C4} bond and allow its S_N2 cleavage by chloride ion. This is followed by cisoid→transoid isomerization and loss of the elements of halogen acid to form the products. In the Lewis acid-catalyzed rapid reaction of 4-phenyl-1,3,3-*tris*-carbethoxycyclobutene in CH_2Cl_2, coordination of Lewis acid with the geminal ester group is followed by heterolytic cleavage of σ_{C3C4} bond. The resultant species subsequently undergoes cisoid→transoid isomerization before losing the Lewis acid to form the products.

KEYWORDS. 1,3,3-*tris*-carbethoxy-4-methylcyclobutene, 1,3,3-*tris*-carbethoxy-4-phenylcyclobutene, torquoselectivity, quantum chemical calculation, heterolytic ring cleavage, solvent effects

---

vijendra@iitk.ac.in

dprasad@iitk.ac.in

arpitayadav@yahoo.co.in

maddali@iitk.ac.in

Introduction. Cyclobutene bearing an electron-donating substituent undergoes conrotatory ring-opening such that the substituent rotates outward to reside *trans* on the π bond.[1–3] There were no known exceptions to this general rule until a research group reported inward rotation of methyl and phenyl substituents from the reactions of **1a** and **1b**, respectively, Scheme 1.[4] A solution of **1a** in $CDCl_3$ was heated to 353 K for 36 h to obtain 4.5:1 mixture of **4a** and **5a**. In comparison, the reaction of **1b** was very facile as it occurred at room temperature in less than 5 min to exclusively form **4b** on mixing the diazo precursor of **1b** with $AgOCOCF_3$ (5 mol%) in CH_2Cl_2 as solvent. The first formed cisoid dienes **2** and **3** isomerized subsequently to the transoid dienes **4** and **5**, respectively, under the reaction conditions. Such cisoid-transoid isomerizations under thermal conditions are common knowledge and routinely practiced in Diels-Alder chemistry.[5]

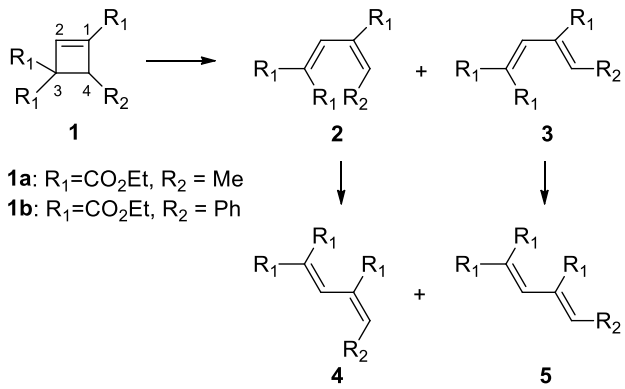

Scheme 1. Inward and outward ring-openings of the cyclobutenes **1a** and **1b**

The previous researchers explained the predominant formation of **4** over **5** as a consequence of thermodynamic control shifted to the cleavage of pyran derivative **6**.[4] The disrotatory 6π electrocyclization[6] **3a**→**6a** and further inward opening **6a**→**2a**, Scheme 2, appeared promising under the reaction conditions because the activation barrier for the transformation **3a**→**6a** was significantly lower than **1a**→**3a**, and the inward opening **6a**→**2a** further lower. It was also discovered that the activation barrier for outward opening **6a**→**3a** was lower than the inward opening **6a**→**2a** in keeping with the rules of torquoselectivity.[7] The cisoid **2a** was estimated to be less stable than **3a** by about 1.0 kcal/mol in contrast to transoid **4a** being more stable than **5a** by, again, 1.0 kcal/mol.

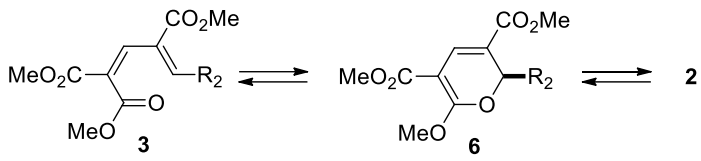

Scheme 2. The 6π electrocyclization of **3**⟶**6** and further opening **6**⟶**2/3**

Thus, **3a** may convert to **6a** soon after it is formed and then **6a** opens outward to **3a** in preference to **2a**. In other words, the transformation **1a**⟶**3a**⟶**6a**⟶**3a** is more facile than **1a**⟶**3a**⟶**6a**⟶**2a**. However, because both the transformations **6a**⟶**3a** and **6a**⟶**2a** take place under significantly high energy conditions required for the initial **1a**⟶**3a** transformation and also because the cisoid-transoid isomerizations **2a**⟶**4a** and **3a**⟶**5a** occur rapidly for being nearly barrier-less, one may invoke larger thermodynamic stability of **4a** over **5a** to allow the former predominate. Attempts to detect the pyran species **6** by NMR, however, failed. Attempt to trap **6** as Diels-Alder cycloadduct with very reactive tetracyanoethylene (TCNE) was also surprisingly not successful. For as long the activation energy of the Diels-Alder reaction is lower than the transformation **1a**⟶**3a**, the trapping experiment need not fail (vide infra). It is important to note that for 1.0 kcal/mol energy difference between **4a** and **5a**, the equilibrium distribution **4a**:**5a** will be estimated at 5:1 at 298 K, which goes well with the experimentally observed 4.5:1 distribution at 353 K. The selectivity is known to generally decrease with the raise in temperature. However, as it will be seen later in the text, the equilibrium ratio **4b**:**5b** cannot be explained in as straightforward a manner as the above **4a**:**5a** distribution.

We report herein that the ring-opening may very well proceed by heterolytic cleavage of $\sigma_{C3\text{-}C4}$ bond which has been rendered labile by the geminal electron-withdrawing ester groups. The heterolytic cleavage is facilitated by the Brønsted acid HCl, adventitious or generated in situ from decomposition of chloroform on heating and also by the Lewis acid $AgOCOCF_3$, added externally to the reaction mixture.

Computational methods. Ethyl ester and D^+ were modelled computationally by methyl ester and H^+, respectively. Geometry optimizations and TS searches were carried out under 1.0 atmosphere pressure at 298 K using the hybrid meta-GGA M06-2X density functional[8] and 6-31G(d) basis set embedded in Gaussian 09.[9] The previous researchers used B3LYP density functional instead, and the same basis set for complete geometry optimizations and transition structure searches. The optimized structures were verified as minima or first order saddle points by harmonic

vibrational frequency analysis. The solvent effects of $CHCl_3$, CH_2Cl_2 and DMSO on reaction profiles were estimated using the Conductor Polarized Continuum Model (CPCM).[10] All the energies reported are Gibbs' Free Energies (sum of electronic and thermal Free Energies). The estimated geometry coordinates, ground state energies, activation energies and single imaginary frequencies of transition structures are given in the Supplementary Information.

Results and Discussion. The outward opening **1**→**3** is significantly lower than inward opening **1**→**2** and, thus, both substrates conform to the rules of TS-torquoselectivity in as much as an electron-donating or electron-rich substituent is required to rotate outward. Having granted that the cisoid-transoid conformational change is nearly barrier-less, transoid **5** must prevail. The experimental result, however, is contradicting because transoid **4** was observed predominantly. The activation energies of the reactions **1**→**2** and **1**→**3** are collected in Table 1.

Table 1. Calculated activation energies (kcal/mol) for ring-openings in **1a** and **1b** in gas phase

Substrate	$\triangle G^{\ddagger}_{(\mathbf{1\rightarrow 2})}$	$\triangle G^{\ddagger}_{(1\rightarrow 3)}$	$\triangle G^{\ddagger}_{(\mathbf{1\rightarrow 2})} - \triangle G^{\ddagger}_{(1\rightarrow 3)}$
1a	37.0	30.9	6.1
1b	33.6	25.4	8.2

The activation energy of the reaction **3a**→**6a** was estimated to be 3.6 kcal/mol lower than **2a**→**6a**. In close analogy, activation energy of the reaction **3b**→**6b** was also 4.1 kcal/mol lower than **2b**→**6b**. Two significant points emerge: (a) The 6π ring-closing reaction **3**→**6** is more facile than **2**→**6**, and (b) both the ring-closing reactions **3**→**6** and **2**→**6** are sufficiently more facile than the first ring-opening reactions **1**→**3** and **1**→**2**, respectively. Thus, both **2** (if any formed at all) and **3** must ring-close to **6** as soon as they are formed. Thus, the TS-torquoselectivity of conrotatory ring-opening in **1** effectively translates into that of disrotatory ring-opening in **6**. The activation energies of the reactions **2**/**3**→**6** are collected in Table 2.

Table 2. Calculated energies of activation (kcal/mol) for 6π ring-closing reactions **2**/**3**→**6** in gas phase

Reaction	$\triangle G^{\ddagger}$
2a→**6a**	18.8
3a→**6a**	15.2
2b→**6b**	21.2
3b→**6b**	17.1

Consequently, we investigated the ring-opening in **6** and discovered that the outward opening reactions **6a**⟶**3a** and **6b**⟶**3b** were 3.7 and 0.6 kcal/mol lower than the corresponding inward opening reactions **6a**⟶**2a** and **6b**⟶**2b**, respectively. These activation energies are collected in Table 3. On putting together the events **1**⟶**2/3**, **2/3**⟶**6** and **6**⟶**2/3**, and also having noted above that **6**⟶**2/3** is the actual torquoselectivity control element in the opening of **1**, **6a**⟶**3a** transformation will predominate over **6a**⟶**2a** for the 3.7 kcal/mol activation energy difference. Likewise, **6b** will be expected to generate approximately 1:3 equilibrium mixture of **2b** and **3b** for the 0.6 kcal/mol activation energy difference. Neither prediction is supported by the experiments. By limiting the argument to formation of the pyran species **6**, the experimental results signal thermodynamic equilibration through reaction reversal as indeed considered by the previous investigators. However, the equilibrium ratio of the products based on ground state energy differences cannot be explained (vide infra). The reaction profiles for the changes **1**⟶**3**⟶**6**⟶**3** are shown in Figure 1.

Table 3. Calculated activation energies (kcal/mol) for 6π ring-opening reactions **6**⟶**2/3**

Reaction	$\Delta G^{\ddagger}$
6a⟶**2a**	20.9
6a⟶**3a**	17.2
6b⟶**2b**	19.6
6b⟶**3b**	19.0

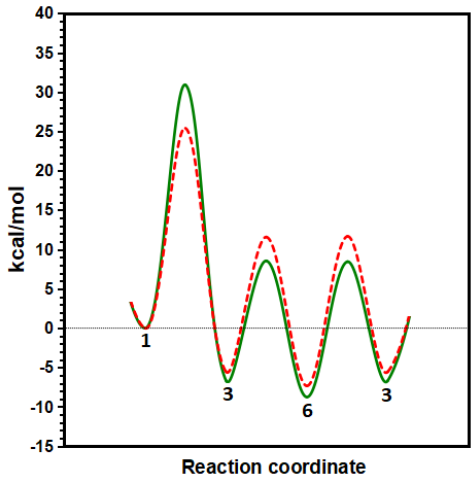

Figure 1. Reaction profiles for the transformations **1a**⟶**3a**⟶**6a**⟶**3a** (solid green line) and **1b**⟶**3b**⟶**6b**⟶**3b** (dotted red line)

As noted above, the previous researchers' attempts at NMR detection of **6** and also its trap as Diels-Alder adduct with TCNE had failed. We wished to understand the reason for this failure and, hence, computed the transition structures for Diels-Alder reaction. The profiles for the reactions of **6a** and **6b** with TCNE are collected in Figure 2. The two reaction profiles are very similar, but with the difference in enthalpy change. While the reaction of **6a** is endergonic by 4.2 kcal/mol, it is 6.4 kcal/mol for **6b**. Both the reactions are, therefore, reversible. Houk has previously succeeded in trapping 1,3-dienes formed from 3-carbomethoxy-1,2-benzocyclobutene and *N*,*N*-dimethy-1,2-benzocyclobutene-3-corboxamide by using, respectively, *N*-phenylmaleimide and maleic anhydride as the other reacting partners.[2b, 11] The openings of these benzocyclobutene derivatives are sufficiently endergonic and, hence, rapidly reversible.[12] Failure to trap the pyran species with TCNE is very surprising. It is likely that the pyran species was not involved at all (vide infra)!

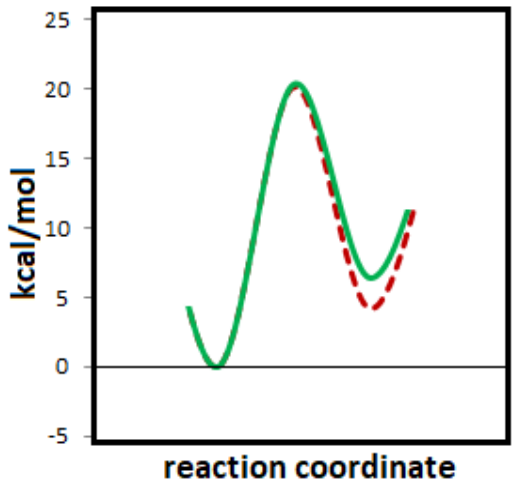

Figure 2. Reaction profiles for the Diels-Alder cycloaddition reactions of **6a** (dotted red line) and **6b** (solid green line) with TCNE

Like the previous investigators, we also casually considered **3**→**2** or **5**→**4** double bond isomerization to understand the predominance of **2** or **4**, respectively. Numerous attempts at locating the TS for **3a**→**2a** isomerization led to the pyran species **6a**. Estimation of activation energy for **5a**→**4a** isomerization always collapsed to either an oxetene (see below) or structures resembling **5a** or **4a** with a very weak vibration elsewhere in the molecule. The issue was resolved

from conformational scan, wherein the torsion angle of the methyl group on π bond with the carbonyl carbon of the ester group on adjacent carbon was varied by 5° at a time, with everything else relaxed, to achieve the highest energy point and then refined around it by 1° change at a time to arrive at $\triangle G^{\ddagger}$ = 61.8 kcal/mol for the isomerization **5a**→**4a**. This value was estimated at 38.4 kcal/mol by the previous investigators. From a similar exercise, $\triangle G^{\ddagger}$ for the π bond isomerization **5b**→**4b** was estimated at 64.0 kcal/mol. These activation energies are too high to compete any of the processes discussed above. Thus, any argument holding **5**→**4** double bond isomerization responsible for the predominant formation of **4** is untenable. In spite of differing estimates of π bond isomerization activation energies, this finding is in line with the predictions of the previous investigators. The estimated reaction profiles for the transformations **1a**→**3a**→**5a**→**4a** and **1b**→**3b**→**5b**→**4b** are shown in Figure 3.

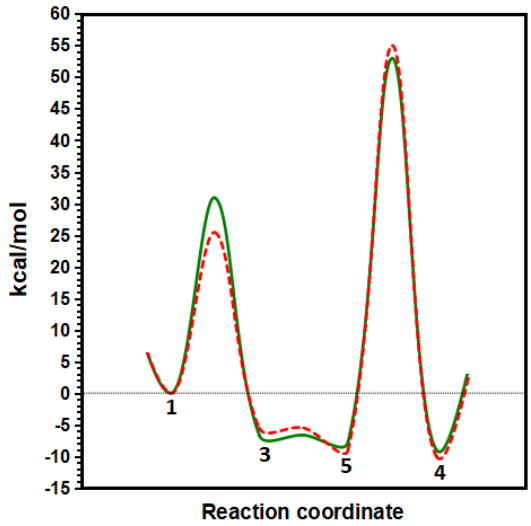

Figure 3. Reaction profiles for the transformations **1a**→**3a**→**5a**→**4a** (solid green line) and **1b**→**3b**→**5b**→**4b** (dotted red line)

The electrocyclization **5a**→**7a**, Scheme 3, followed by conrotatory opening in **7a** was investigated for the first time as a possibility. The outward opening **7a**→**4a** ($\triangle G^{\ddagger}$ = 18.9 kcal/mol) is favored over inward opening **7a**→**5a** ($\triangle G^{\ddagger}$ = 24.8 kcal/mol). Also, while both these openings are possible under the reaction conditions, the activation energy of the initial **5a**→**7a** transformation, 55.7 kcal/mol, is way above the activation energies of **1a**→**2a**/**3a** transformations. The activation energy for the transformation **3a**→**7a** is 49.2 kcal/mol. Though

tantalizingly on the predominant experimental product by the conrotatory pathway, very high activation energies for **5a**→**7a** and **3a**→**7a** transformations preclude the oxetene pathway. The reaction profiles for the transformations **7a**→**4a** and **7a**→**5a** are collected in Figure 4.

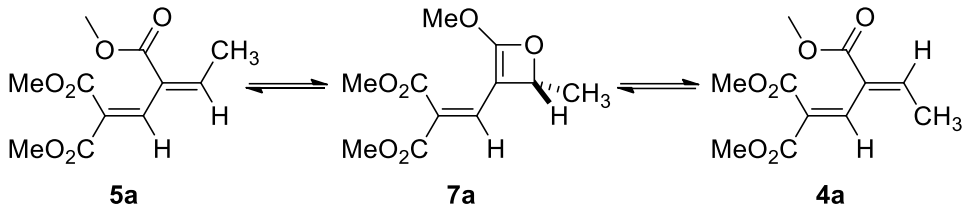

Scheme 3. Four-electron ring-closing reaction **5a**→**7a** and the ring-opening reactions **7a**→**4a** and **7a**→**5a**

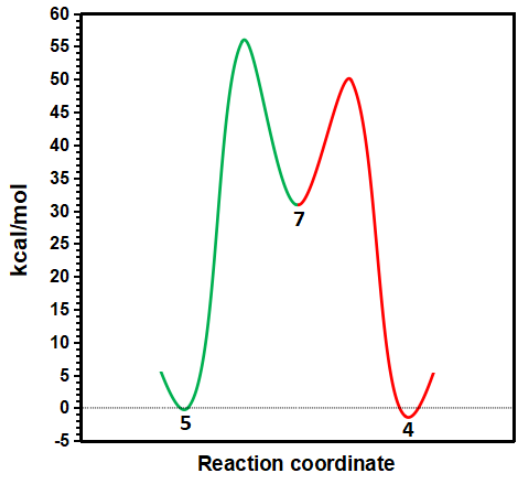

Figure 4. Reaction profiles for the transformations **7a**→**5a** (green line) and **7a**→**4a** (red line)

The hyperconjugative electron donating methyl group on one end and resonance accepting geminal ester groups on the other must weaken $\sigma_{C3\text{-}C4}$ bond in **1a** to allow its facile S_N2 cleavage. Additionally, protonation of a geminal ester group will render the σ_{C3C4} bond further weak and, thus, the said S_N2 cleavage smoother. Indeed, on carbonyl protonation, $\sigma_{C3\text{-}C4}$ bond length changes from 1.58 Å to 1.60 Å in the gas phase and also under the solvent effects of $CHCl_3$. Likewise, $\sigma_{C3\text{-}C4}$ bond in **1b** changes from 1.59 Å to 1.61 Å in the gas phase and also under the solvent effects of DMSO. In **1b**, strong cation-stabilizing ability of the phenyl group may encourage even heterolytic cleavage of $\sigma_{C3\text{-}C4}$ bond on coordination of a geminal ester group to Lewis acids. With these concepts, we proceeded to investigate the reactions of **1a** and **1b**.

DCl, adventitious or generated in situ from $CDCl_3$ on heating,[13] may conceivably protonate a geminal ester group and allow S_N2 cleavage of σ_{C3C4} bond by chloride ion to the species **8** and **9** after cisoid→transoid isomerization, as shown in Scheme 4. The species **8** reorganizes by losing the elements of DCl in the manner shown to form the predominantly observed product **4a**. The conformer **9** will form the minor product **5a**.

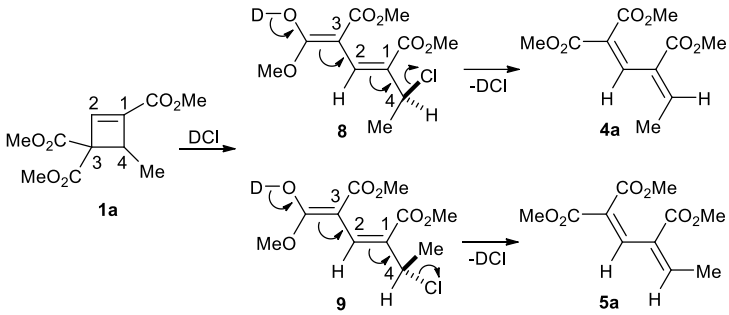

Scheme 4. Proposed cleavage of **1a** under DCl-catalysis

The stereoelectronic effect[14] requires $\sigma_{C\text{-}Cl}$ bond align parallel to the *p* orbitals of the diene system for maximum overlap to cause elimination of DCl from **8** and **9**. These conformations actually resemble the transition structures for elimination. Indeed, after having constrained the geometry by fixing the torsion angle C2-C1-C4-Cl at 90°, the conformer **8*** was estimated to be 1.0 kcal/mol more stable than **9*** under the solvent effect of chloroform at 298 K. The energy difference translates to **8***:**9*** = 5.4:1 equilibrium distribution. Having assumed that the facility for DCl elimination from both the species is equal, the resultant **4a**:**5a** distribution will also be the same and lower, close to the experimental 4.5:1 distribution, on temperature correction.[15] Geometries of **8*** and **9*** are given in the Supplementary Information.

It is interesting to note that with no restriction on C2-C1-C4-Cl torsion angle, the species **8** is less stable than **9** by 0.22 kcal/mol under the solvent effects of $CHCl_3$. It is only on imposition of the torsion angle constraint required for DCl elimination that the relative stability reversed. Thus, the solvent and definitive transition structure geometry requirement play crucial roles in product composition determination.[16]

The $\triangle G^{\ddagger}$ for nucleophilic cleavage of protonated-**1a** (**1a**-H^{+}) by chloride ion was estimated at -72.4 kcal/mol (Imaginary Frequency = -446.2) in the gas phase. Such a reaction profile with negative activation energy is common for S_N2 reactions.[17] On including the solvent effects of chloroform, $\triangle G^{\ddagger}$ was estimated at 3.0 kcal/mol (Imaginary Frequency = -447.6). This energy requirement is too small to impede the reaction. The ring cleavage is >39.0 kcal/mol exergonic. The reaction profiles for the reaction of **1a**-H^{+} to relaxed **8** and **9** and then torsion angle constrained **8*** and **9*** under the solvent effects of $CHCl_3$ are given in Figure 5.

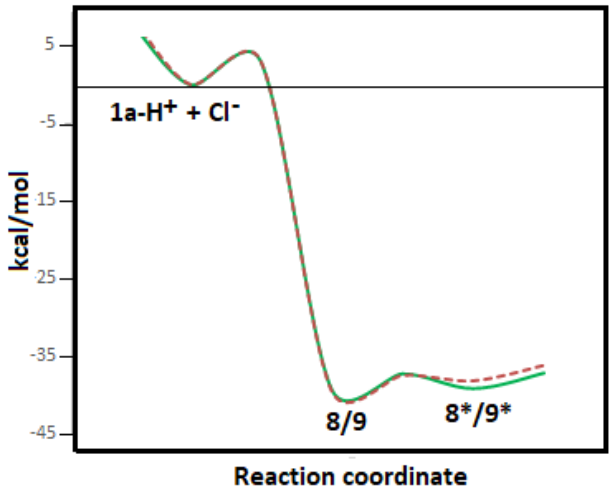

Figure 5. Profile for the reaction of **1a**-H^{+} with chloride ion leading to **8** (solid green line) and **9** (broken red line) and the corresponding torsion angle constrained structures **8*** and **9*** under the solvent effects of chloroform

The ring-opening in **1b** was very facile as it occurred at room temperature in less than 5 min to exclusively form **4b** on mixing with 5 mol% $AgOCOCF_3$, a Lewis acid, in CH_2Cl_2 as the reaction solvent. The heterolytic cleavage of σ_{C3C4} bond after coordination of a geminal ester group with the Lewis acid to generate the zwitter ions **10** and **11**, Scheme 5, will be expected to be rapid for the benzylic nature of the cation. However, the large steric interaction of the phenyl group with the adjacent ester group in **11** may guarantee bias for the zwitter ion **10** and, thus, lead exclusively to **4b** on loss of the Lewis acid.

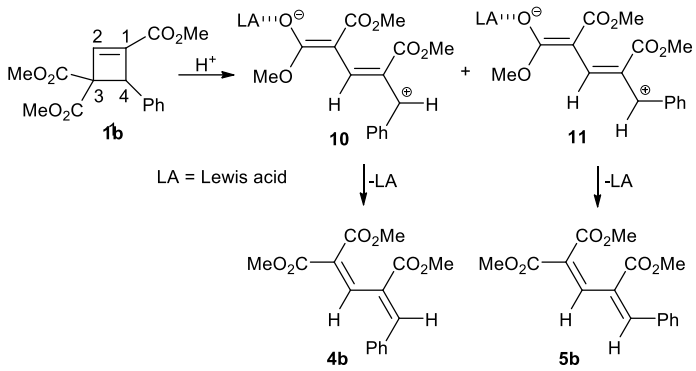

Scheme 5. Lewis acid-catalysed cleavage of **1b** leading to **4b** and **5b**

We have computationally modelled the Lewis acid $AgOCOCF_3$ by H^+ and discovered that the species **10** is indeed more stable than **11** by 3.62 kcal/mol under the solvent effects of CH_2Cl_2. This energy difference predicts exclusive formation of **10** and, thus, **4b** as indeed observed experimentally. The computed 3D geometries of **10** and **11** are given in the Supplementary Information.

Thus, we indeed have alternate routes to the predominant formation of **4a** and **4b** from the reactions of **1a** and **1b**, respectively, following pathways that are significantly lower in energy compared to the usual conrotatory ring opening. The reactions involve protonation or Lewis acid coordination of a geminal ester group followed by S_N2 cleavage of the ring bond in **1a** and heterolysis in **1b**.

The previous investigators have also reported that when either **1a** or 4.5:1 mixture of the dienes **4a** and **5a** was heated in DMSO-*d*6 at 353 K for 12 h, a 3:1 mixture of **4a**:**5a** was obtained. Following the rules of TS-torquoselectivity, **1a** is estimated to prefer outward to inward opening by a margin of 7.0 kcal/mol under the solvent effects of DMSO. Therefore, the change in concentration of inward product in this instance also requires an explanation. It is significant to note that **4a** is more stable than **5a** by 0.5 kcal/mol under the solvent effects of DMSO. This energy difference corresponds to **4a**:**5a** = 2.3:1 equilibrium distribution at 298 K, expected to lower at 353 K. The observed 3:1 distribution therefore does not support the proposed

thermodynamics-driven equilibration. The reaction profiles for the openings of **1a** in DMSO are given in Figure 6.

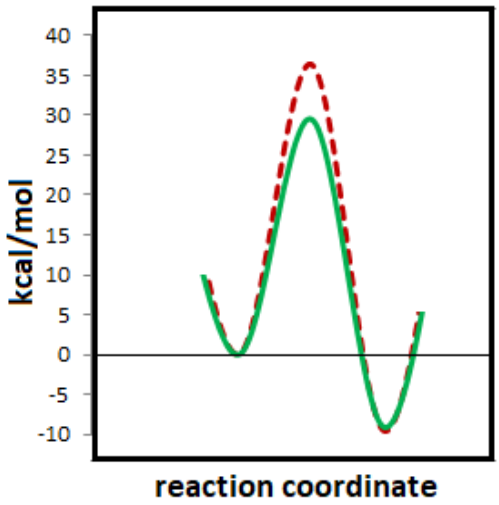

Figure 6. Reaction profiles for the transformations **1a**→**2a**/**4a** (dotted red line) and **1a**→**3a**/**5a** (solid green line) under the solvent effects of DMSO

Under the solvent effects of DMSO, the outward opening **6a**→**3a/5a** is 3.0 kcal/mol more facile than inward opening **6a**→**2a/4a**. This energy difference was 3.7 kcal/mol in the gas phase calculations. Thus, the lessons learnt from gas phase calculations are also valid under the solvent effects of DMSO. The reaction profiles are given in Figure 7.

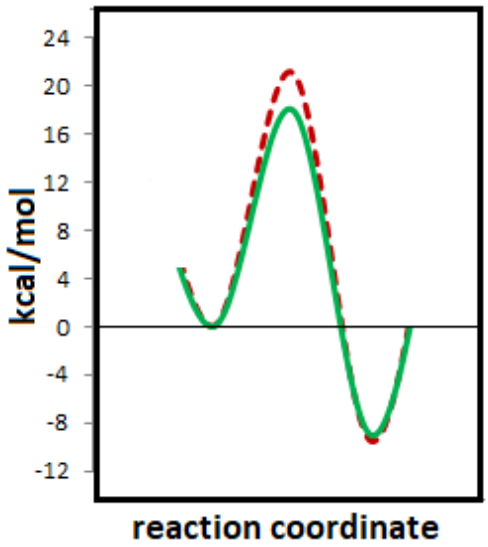

Figure 7. Reaction profiles for the transformations **6a**→**2a**/**4a** (dotted red line) and **6a**→**3a**/**5a** (solid green line) under the solvent effects of DMSO

DMSO is a nucleophilic solvent.[18] Analogous to ring-opening by chloride ion, S_N2 attack of DMSO at elevated temperature (353 K) may open the ring to form the dienolates **12** and **13** after cisoid→transoid isomerization as shown in Scheme 6. Like in **8** and **9**, the torsion angle-constrained conformer **12** is 0.9 kcal/mol more stable than **13** under the solvent effects of DMSO at 298 K. This energy difference corresponds to 4.6:1 distribution of **12**:**13** and, hence, also **4a**:**5a**. This distribution will also lower and match better with the experimental 3:1 distribution at the experimental 353 K temperature. DMSO can also add to the dienes **4** and **5** in conjugate manner to generate the same species **12** and **13**. The previous researchers did not comment on the ratio **4a**:**5a** that changed from 4.5:1 to 3:1 on heating in DMSO.

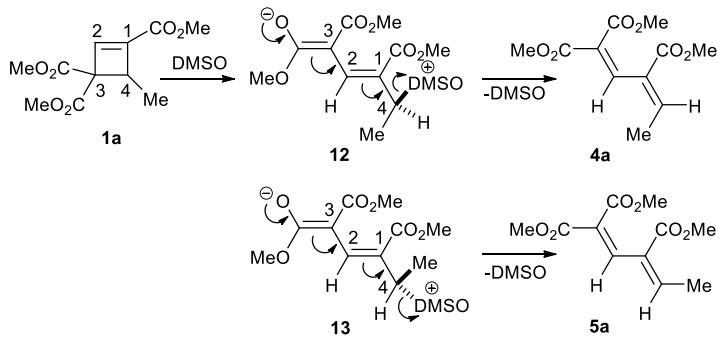

Scheme 6. DMSO-initiated S_N2 cleavage pathway to **4a** and **5a**

Conclusion. The ring-opening of **1** is argued to alternatively follow a heterolytic pathway under electron-withdrawing effect of the geminal ester groups on one end and electron-releasing methyl group on the other end of the cleaving ring bond rather than the usual conrotatory pathway following the rules of torquoselectivity. The reaction of **1a** is catalyzed by the adventitious or in situ generated DCl from $CDCl_3$ on heating at 353 K over 36 h. Protonation of a geminal ester group weakens σ_{C3C4} bond and allows its smooth S_N2 cleavage by chloride ion. This is followed by cisoid→transoid isomerization and elimination of the elements of DCl under stereoelectronic control to form the products.

In the instance of **1b**, the ring opens on coordination of $AgOCOCF_3$ to the geminal ester group. The resultant cation is benzylic and, thus, sufficiently stable. This is followed by cisoid→transoid isomerization and loss of $AgOCOCF_3$ under stereoelectronic control to form the products.

The transformation of **1a** into 3:1 mixture of **4a**:**5a** on heating for 12 h in DMSO at 353 K is also argued to proceed by heterolytic S_N2 ring cleavage by DMSO to result in dienolates. The same dienolates may also form from conjugate addition of DMSO to the dienes **4a** and **5a**. These dienolates then eject DMSO under stereoelectronic control to form a mixture of **4a** and **5a**.

Overall, both the reactions are argued to proceed via heterolytic ring-cleavage under the combined steric control of methyl or phenyl substituent and the ester group on adjacent carbon. The rules of torquoselectivity, therefore, need not apply to the substrates **1a** and **1b** because they react by heterolytic pathways rather than the usual conrotatory ring-opening.

ASSOCIATED CONTENT

Supporting Information

Coordinates of the geometries, Gibbs' Free Energies, Gibbs' Activation Free Energies, and imaginary frequencies of the transition state structures

AUTHOR INFORMATION

Corresponding Author

vijendra@iitk.ac.in

Notes

The authors declare no competing financial interests.

ACKNOWLEDGMENT

VKY thanks the Council of Scientific & Industrial Research, Government of India, for financial support. The authors acknowledge allocation of time on HPC2013 series of supercomputers by the Computer Centre of IIT Kanpur.

REFERENCES

1. (a) Woodward, R. B.; Hoffmann, R. *J. Am. Chem. Soc.* **1965**, *87*, 395−397. (b) Hoffmann, R.; Woodward, R. B. *Acc. Chem Res.* **1968**, *1*, 17−22.
2. (a) Rondan, N. G.; Houk, K. N. *J. Am. Chem. Soc.* **1985**, *107*, 2099−2111. (b) Niwayama, S.; Kallel, E. A.; Spellmeyer, D. C.; Sheu, C.; Houk, K. N. *J. Org. Chem.* **1996**, *61*, 2813−2825.
3. For examples of outward rotation of 3-phenyl group, see: (a) Murakami, M.; Miyamoto, Y.; Ito, Y. *J. Am. Chem. Soc.* **2001**, *123*, 6441–6442. (b) Shindo, M.; Matsumoto, K.; Mori, S.; Shishido, K. *J. Am. Chem. Soc.* **2002**, *124*, 6840–6841. (c) Shindo, M.; Sato, Y.; Yoshikawa, T.; Koretsune, R.; Shishido, K. *J. Org. Chem.* **2004**, *69*, 3912–3916.
4. Um, J. M.; Xu, H.; Houk, K. N.; Tang, W. *J. Am. Chem. Soc.* **2009**, *131*, 6664−6665.
5. (a) Nicolaou, K. C.; Snyder, S. A.; Montagnon, T.; Vassilikogiannakis, G. *Angew. Chem. Int. Ed.* **2002**, *41*, 1668−1698. (b) Hayashi, Y.; Samanta, S.; Gotoh, H.; Ishikawa, H. *Angew. Chem. Int. Ed.* **2008**, *47*, 6634−6637. (c) Nakashima, D.; Yamamoto H. *J. Am. Chem. Soc.* **2006**, *128*, 9626−9627. (d) Dockendorff, C.; Sahli, S.; Olsen, M.; Milhau, L.; Lautens, M. *J. Am. Chem. Soc.*, **2005**, *127*, 15028−15029.
6. (a) Evanseck, J. D.; Thomas, B. E.; Spellmeyer, D. C.; Houk, K. N. *J. Org. Chem.* **1995**, *60*, 7134−7141. (b) Akerling, Z. R.; Norton, J. E.; Houk, K. N. *Org. Lett.* **2004**, *6*, 4273−4275.
7. For an account of the seminal work of K. N. Houk on torquoselectivity, see: (a) Kirmse, W.; Rondan, N. G.; Houk, K. N. *J. Am. Chem. Soc.* **1984**, *106*, 7989−7991. (b) Houk, K. N.; Spellmeyer, D. C.; Jefford, C. W.; Rimbault, C. G.; Wang, Y.; Miller, R. D. *J. Org. Chem.* **1988**, *53*, 2125−2127.
8. (a) Zhao Y.; Truhlar, D. G. *Acc. Chem. Res.* **2008**, *41*, 157−167. (b) Bursch, M.; Caldeweyher, E.; Hansen, A.; Neugebauer, H.; S. Ehlert, S.; Grimme, S. *Acc. Chem. Res.* **2019**, *52*, 258−266. (c) Caldeweyher, E.; Mewes, J.-M.; Ehlert S.; Grimme, S. *Phys. Chem. Chem. Phys.* **2020**, *22*, 8499−8512. (d) Deng, Q.; Mu, F.; Qiao, Y.; Wei, D. *Org. Biomol. Chem.* **2020**, *18*, 6781−6800.
9. Gaussian 09, Revision B.01, Frisch, M. J.; Trucks, G. W.; Schlegel, H. B.; Scuseria, G. E.; Robb, M. A.; Cheeseman, J. R.; Scalmani, G.; Barone, V.; Mennucci, B.; Peterson, G. A.; Nakatsuji, H.; Caricato, M.; Li, X.; Hratchian, H. P.; Izmaylov, A. F.; Bloino, J.; Zheng, G.; Sonnenberg, J. L.; Hada, M.; Ehara, M.; Toyota, K.; Fukuda, R.; Hasegawa, J.; Ishida, M.; Nakajima, T.; Honda, Y.; Kitao, O.; Nakai, H.; Vreven, T.; Montgomery, Jr., J. A.; Peralta, J. E.; Ogliaro, F.; Bearpark, M.; Heyd, J. J.; Brothers, E.; Kudin,K. N.; Staroverov, V. N.; Keith, T.; Kobayashi,R.;Normand, J.; Raghavachari, K.; Rendell, A.; Burant, J. C.; Iyengar, S. S.; Tomasi, J.; Cossi, M.; Rega, N.; Millam, J. M.; Klene, M.; Knox, J. E.; Cross, J. B.; Bakken, V.; Adamo, C.; Jaramillo, J.; Gomperts, R.; Stratmann, R. E.; Yazyev,

O.; Austin, A. J.; Cammi, R.; Pomelli, C.; Ochterski, J. W.; Martin, R. L.; Morokuma, K.; Zakrzewski, V. G.; Voth, G. A.; Salvador, P.; Dannenberg, J. J.; Dapprich, S.; Daniels, A. D.; Farkas, O.; Foresman, J. B.; Ortiz, J. V.; Cioslowski, J.; Fox, D. J. Gaussian, Inc., Wallingford CT, 2010.

10. (a) Barone, V.; Cossi, M. *J. Phys. Chem.* A, **1998**, *102*, 1995−2001. (b) Cossi, M.; Rega, N.; Scalmani, G.; Barone, V. *J. Comput. Chem.* **2003**, *24*, 669−681.
11. Jefford, C. W.; Bernardinelli, G.; Wang, Y.; Spellmeyer, D. C.; Buda, A.; Houk, K. N. *J. Am. Chem. Soc.* **1992**, *114*, 1157.
12. We have previously calculated many double bond isomerizations and found the activation energies significantly high. See: Yadav, A.; Prasad, D. L. V. K.; Yadav, V. K. (**2017**): ChemRxiv. Preprint. https://doi.org/10.26434/chemrxiv.5743305.v1
13. (a) Deslongchamps, P. in Stereoelectronic Effects in Organic Chemistry, Pergamon press, 1983. (b) Yadav, V. K. in Steric and Stereoelectronic Effects in Organic Chemistry, Springer, 2016.
14. (a) Zhu, L.; Bozzelli, J. W. *Int. J. Chem. Kinet.* **2003**, *35*, 647-660. (b) Chan, A. M.; Peña, L. A.; Segura, R. E.; Auroprem, R.; Harvey, B. M.; Brooke, C. M.; Hoggard, P. E. *Photochem. Photobiol.* **2013**, *89*, 274–279.
15. (a) Stone, G. B. *Tetrahedron: Asymmetry* **1994**, *5*, 465–472. (b) Phillips, R. S.; Zheng, C.; Pham, V. T.; Andrade, F. A. C.; Andrade, M. A. C. *Biocatalysis* **1994**, *10*, 77–86. (c) Cainelli, G.; Giacomini, D.; Galletti, P. *Chem. Commun.* **1999**, 567–572. (d) Poon, T.; Sivaguru, J.; Franz, R.; Jockusch, S.; Martinez, C.; Washington, I.; Adam, W.; Inoue, Y.; Turro, N. J. *J. Am. Chem. Soc.* **2004**, *126*, 10498–10499. (e) Abe, M.; Terazawa, M.; Nozaki, K.; Masuyama, A.; Hayashi, T. *Tetrahedron Lett.* **2006**, *47*, 2527–2530. (f) Cainelli, G.; Galletti, P.; Giacomini, D. *Chem. Soc. Rev.* **2009**, ***38***, 990–1001. (g) Parker, J.; Novakovic, K. *ChemPhysChem* **2017**, *18*, 1981–1986. (h) Yadav, V. K.; Prasad, D. L. V. K.; Yadav, A.; Yadav, K. *J. Phys. Org. Chem.* **2020** (DOI: 10.1002/poc.4131)
16. Saadat, K.; Lopez, R. V.; Shiri, A.; Faza, O. N.; Lopez, C. S. *Org. Biomol. Chem.* **2020**, *18*, 6287–6296.
17. For negative energies of activation for S_N2 reactions, see: (a) Stei, M.; Carrascosa, E.; Kainz, M. A.; Kelkar, A. H.; Meyer, J.; Szabó, I.; Czakó, G.; Wester, R. *Nat. Chem.* **2016**, *8*, 151–156. (b) Xie, J.; Hase, W. L. *Science* **2016**, *352*, 32–33. (c) Wang, Y.; Song, H.; Szabóa, I.; Czakó, G.; Guo, H.; Yang, M. *J. Phys. Chem. Lett.*, **2016**, *7*, 3322–3327. (d) Szabóa, I.; Czakó, G. *J. Phys. Chem.* A **2017**, *121*, 9005−9019. (e) Hamlin, T. A.; Swart, M.; Bickelhaupt, F. M. *ChemPhysChem* **2018**, *19*, 1315–1330.
18. (a) Kornblum, N.; Powers, J. W.; Anderson, G. J.; Jones, W. J.; Larson, H. O.; Levand, O.; Weaver, W. M. *J. Am. Chem. Soc.* **1957**, *79*, 6562. (b) Epstein, W. W.; Sweat, F. W. *Chemical Reviews* **1967**, *67*, 247–260. (c) Tidwell, T. T. *Synthesis*. **1990**, 857–870.

For Table of Contents

The transformations of 4-methyl- and 4-phenyl-1,3,3-*tris*-carbethoxycyclobutenes to s-*trans*-*trans*-1,1,3-*tris*-carbethoxy-4-methyl-1,3-butadiene and 4-phenyl-1,3-butadiene, respectively, proceed through heterolytic cleavage of the σ_{C3C4} bond rather than the usual four-electron conrotatory ring opening.